SMiRT-12 / K. Kussmaul (Editor)

FG14/2

PREDICTION OF CRACK PROPAGATION IN TYPE 304 STAINLESS STEEL CYLINDRICAL SPECIMENS SUBJECTED TO CYCLIC THERMAL LOADS

T. Fujioka, Y. Takahasi, Y. Satoh and Y. Fukuda

ABSTRACT

A simple method for predicting thermal fatigue crack propagation in inelastic situation is described in this paper along with its experimental validation. The method is based on a combination of elastic thermal stress analysis of the uncracked body with stress intensity factor solutions, thus can be easily employed for practical use, where appropriate sensitivity analyses should be performed. The experimental validation has been performed by comparing crack propagation predictions with results of thermal fatigue tests using cylindrical specimens which contained semi-elliptical surface pre-notches.

1 INTRODUCTION

As a result of a collaborative study on high-temperature flaw assessment procedures between the Electric Power Research Institute (EPRI) in the US, Nuclear Electric (NE) in the UK and the Central Research Institute of Electric Power Industry (CRIEPI) in Japan, an interim flaw assessment procedure for high-temperature reactor components was presented [1]. After the presentation of the interim procedure, efforts to improve or validate the proposed methodologies incorporated in the procedure have been continued as a phase-II collaboration between NE and CRIEPI, and a revised flaw assessment guide has been presented [2] as well as the phase-II final report [3].

This paper describes one of the continued studies concerning thermal fatigue crack propagation prediction along with its experimental validation. The proposed assessment guide allows the use of a combination of elastic stress analysis of the uncracked body with stress intensity factor solutions. Since this simple method is based on linear fracture mechanics, it can be easily employed for practical use, where appropriate sensitivity analyses should be performed. Numerical validation of the method has been separately examined by performing inelastic finite element analyses of cracked bodies [4].

The experimental validation described here has been performed by predicting crack propagation in thermal fatigue tests using cylindrical specimens which contained semi-elliptical surface pre-notches. The specimens were subjected to cyclic inelastic deformation. Nevertheless the predictions agreed well with the test results.

2 THERMAL FATIGUE CRACK PROPAGATION TEST

2.1 SPECIMEN

Type 304 stainless steel cylindrical specimens were used for the tests. The outer diameter and the wall thickness of the specimen were 160 and 15 mm,

respectively. Each specimen contained two pre-notched cross sections (indicated as section A-A' and section B-B'), and six surface pre-notches had been introduced by electric spark machining in each section in advance of performing the test (see Fig. 1).

2.2 TEST APPARATUS

Fig. 2 shows the test apparatus with details of the thermally loaded portion of the specimen. Thermal loads are applied to the specimens by contacting two liquid metal plena which are heated to specified temperatures. The plena are contained in a thermally insulated chamber which can be moved up and down by an actuator according to a specified pattern.

In the present tests, the temperature of the liquid metal in the upper plenum was kept at 550°C (hot plenum), and the lower at 150°C (cold plenum), as shown in Fig. 2.

2.3 THERMAL LOADS

Two specimens were thermally loaded by different types of thermal transient conditions. Fig. 3 (a) and Fig. 3 (b) show the chamber movement wave patterns employed in the tests performed, describing the location of the middle of the chamber, z, as functions of time (see also Fig. 3 (c)).

The wave in Fig. 3 (a) caused a sudden drop in temperature after a high temperature hold at 550°C, the other wave in Fig. 3 (b) is the inverse of the former test. Therefore the former test is indicated as the cold shock test in this paper, and the latter as the hot shock test. Since the origin of z was located 20 mm above the middle between the two pre-notched sections, the two waves were not exactly symmetrical with each other for the notches. Each test was conducted until 1000 cycles of the thermal shock were applied.

2.4 TEST RESULTS

By the time surface crack lengths were measured after 500 cycles of thermal shock by replicating the pre-notched surface, thermal fatigue cracks had been initiated at all the outer surface pre-notch roots in the both specimens while any of the inner surface pre-notches showed little crack initiation. After completing the tests, lengths and depths of all the notches were examined by cutting the specimens at the pre-notched sections.

The cold shock test produced obvious thermal fatigue crack propagation from the outer surface pre-notches in the section B-B', while the remainder of the notches showed little or no crack propagation.

Different from the cold shock test, the hot shock test produced significant thermal fatigue crack propagation from the outer surface pre-notches in the section A-A', while the remainder showed little difference from their initial dimensions. Details of the tests are described in a previous report [5].

3 THERMAL FATIGUE CRACK PROPAGATION PREDICTION PROCEDURE

3.1 TEMPERATURE & STRESS HISTORY

To determine histories of temperature and stress of a component to be assessed, finite element analysis is usually employed. However, the analysis of crack containing components can be impractically complicated, especially when three-dimensional cracks are contained in the component.

The flaw assessment guide presented in [2] allows the use of stress analysis of the uncracked component. When the stress history of the uncracked body can be used, it is not necessary to perform stress analysis for several crack dimensions. In this paper, both temperature and stress histories are determined by performing axi-symmetric finite element analyses of the uncracked specimen configuration (see Fig. 1 (a)).

Although the guide allows the use of inelastic strain and stress distributions in the uncracked body [6] for more detailed assessments, this

paper employs purely elastic stress analysis for simplicity and conservativeness in J-integral assessments for a wide range of temperature distribution conditions [4].

Fig. 4 and Fig. 5 show stress distributions for the pre-notched sections obtained from the finite element analyses assuming the boundary condition changes according to the specified chamber movement patterns. The results for the cold shock test are shown in Fig. 4, and in Fig. 5 for the hot shock test. From these figures, stress ranges on the outer surface exceed twice the yield stress, σ_y, which is about 96 MPa for the material at the maximum temperature of 550°C, thus the specimens tested were supposed to have been subjected to significant inelastic deformation. Steady state stresses during the high temperature hold in the cold shock test have proved to be low enough to neglect creep contributions to crack propagation (see Fig. 4).

Consistent with the absence of crack propagation in the tests, stress ranges for the inner surfaces are relatively small (see Fig. 4), thus the inner surface pre-notches are not evaluated in this paper. Further details of the analyses are described in the final report [3].

3.2 STRESS INTENSITY FACTOR

Non-linear stress distributions in Fig. 4 or Fig. 5 can be approximated by the following polynomial equation:

$$\sigma_z(r) = \sigma_o(A_o + A_1 r + A_2 r^2 + A_3 r^3 + \cdots) \tag{1}$$

where $\sigma_z(r)$ is the axial stress component as a function of the radius distance, r, and σ_o is a unit stress. Coefficients, A_o, A_1, ... are determined as functions of time to approximate the stress distributions obtained from the finite element analyses.

If the stress intensity factor, K_i, for each unit stress distribution, $\sigma_o r^i$, is available, the total stress intensity factor, K, for the above stress distribution of Eq. (1) is estimated as:

$$K = A_o K_o + A_1 K_1 + A_2 K_2 + A_3 K_3 + \cdots \tag{2}$$

In this paper, Shiratori's table for dimensionless stress intensity factors for semi-elliptical surface cracks in a plate subjected to unit stress distributions [7] is employed for this procedure, and cubic polynomial approximations are performed.

3.3 FATIGUE J-INTEGRAL RANGE

When the stress changes are mostly caused by thermal loads, and the stress history is calculated by purely elastic analysis, the fatigue J-integral range, ΔJ_f, is conservatively estimated by the following:

$$\Delta J_f = \frac{(\Delta K)^2}{E'} \tag{3}$$

where ΔK is the stress intensity factor range calculated by the above described elastic-based procedures. ΔK is simply determined as the difference:

$$\Delta K = K_{max} - K_{min} \tag{4}$$

where K_{max} is the maximum stress intensity factor for the given stress distribution change and K_{min} is the minimum of K.

Even when the calculated K_{max} is negative, the value should be used for this problem, because the actual K_{max} in the thermally loaded elastic-plastic body can become positive under cyclic inelastic deformation.

Assuming plane stress conditions the material constant E' should be equated to Young's modulus, E, to estimate crack propagation in the crack length direction, while plane strain conditions, $E' = E/(1-\nu^2)$, should be assumed for the depth direction. ν is Poisson's ratio of the material. When the actual value of E changes during a thermal cycle due to its temperature dependency, the lowest value (E at the maximum temperature) should be used in Eq. (3) to obtain conservative assessments of ΔJ_f.

3.4 CRACK PROPAGATION LAW

The following power law type crack propagation law is employed to estimate crack propagation per cycle, da/dN:

$$da/dN = C(\Delta J_f)^l \qquad (5)$$

where the material constants C and l can be determined by referring to material test data.

Separately performed crack propagation tests using center cracked panel specimens of the same material provided values of 9.64×10^{-5} and 1.44 for C and l, respectively, for the evaluation of the cylindrical specimens, where the unit of ΔJ_f is kN/m and da/dN is given in mm/cycle.

4 RESULTS & DISCUSSIONS

Fig. 6 shows the predicted crack propagation after 1000 cycles of thermal shock compared with the test observations. From this figure, the predictions by the proposed method agreed well with the test observations when crack propagation was significant.

Disagreements between the predictions and the tests are seen for the notches where crack propagation was small (notches in the section A-A' of the cold shock test and AO3 in the hot shock test). These disagreements are thought to be caused by the presence of a fatigue crack initiation life at the pre-notch roots.

5 CONCLUSION

Following the flaw assessment guide which has been presented as a result of a collaborative study between NE and CRIEPI, it is possible to predict thermal fatigue crack propagation in inelastic situation. In this paper the validity of the proposed method, which is based on elastic stress analysis of the uncracked body, has been examined by comparing the predictions with test results. The method has been shown to give good predictions in spite of its simplicity.

ACKNOWLEDGEMENT

The authors would like to express their sincere gratitudes to
Dr. R. A. Ainsworth and Dr. P. J. Budden of Berkeley Technology Centre, Nuclear Electric, plc. for valuable discussions.

REFERENCES

[1] Ainsworth, R. A., Ruggles, M. B. and Takahashi, Y. 1992. Flaw Assessment Procedure for High-Temperature Reactor Components. Transactions of ASME, Journal of Pressure Vessel Technology, 114: pp. 166-170.

[2] Ainsworth, R. A. and Takahashi, Y. 1992. Flaw Assessment Guide for High Temperature Reactor Components Subjected to Creep-fatigue Loading. Nuclear Electric Report, Technology Division, Nuclear Electric, TD/SEB/REP/4062/92.

[3] Takahashi, Y. and Ainsworth, R. A. 1993. High-Temperature Flaw Assessment Procedure Phase-II Final Report. CRIEPI Report, Central Research Institute of Electric Power Industry (to be published).

[4] Takahashi, Y. 1993. Study on Simplified Estimation of J-integral under Thermal Loading. Transactions of SMiRT12, L01/5 (to be published).
[5] Takahashi, Y., Ogata, T., Fukuda, Y. and Satoh, Y. 1989. Interim Report of Study on High-Temperature Flaw Assessment Procedure. CRIEPI Report, Central Research Institute of Electric Power Industry, ET89004: pp.25-31.
[6] Budden, P. J. 1989. Fracture Assessment of Combined Thermal and Mechanical Loads Using Uncracked Body Stress Analysis. CEGB Report, Central Electricity Generating Board, RD/B/6158/R89
[7] Shiratori, M. 1986. Analysis of Stress Intensity Factors for Surface Cracks Subjected to Arbitrarily Distributed Stresses. Bulletin of the Faculty of Engineering, Yokohama National University, 35: pp. 1-25.

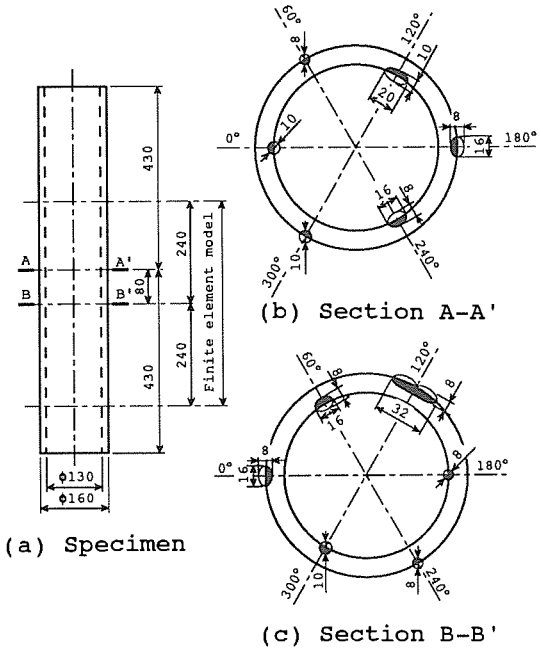

Fig. 1. Dimensions of specimen and pre-notches

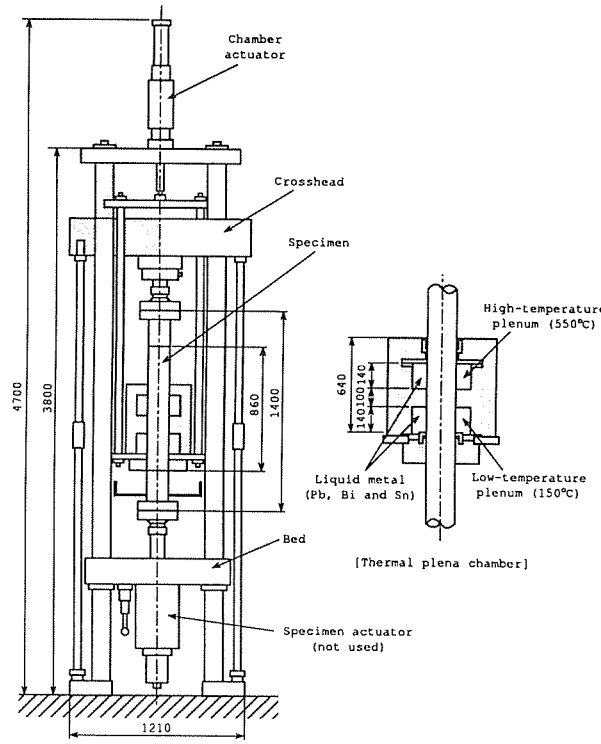

Fig. 2. Thermal fatigue test apparatus

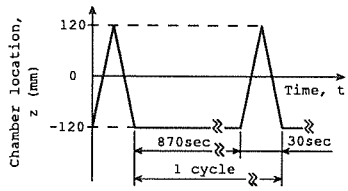

(a) Cold shock test

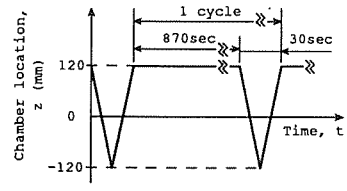

(b) Hot shock test

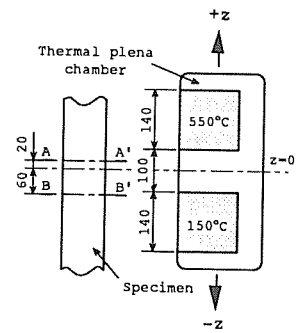

(c) Status at neutral position (z=0)

Fig. 3. Thermal plena chamber movement pattern

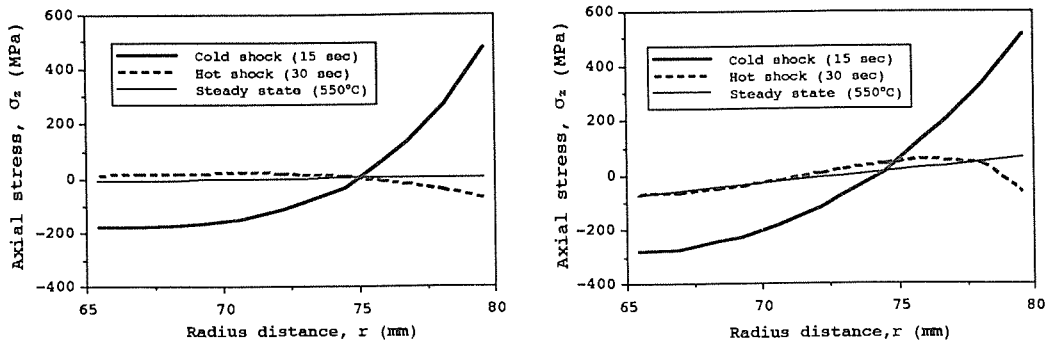

Fig. 4. Stress distribution changes obtained from elastic thermal stress analysis for the cold shock test conditions

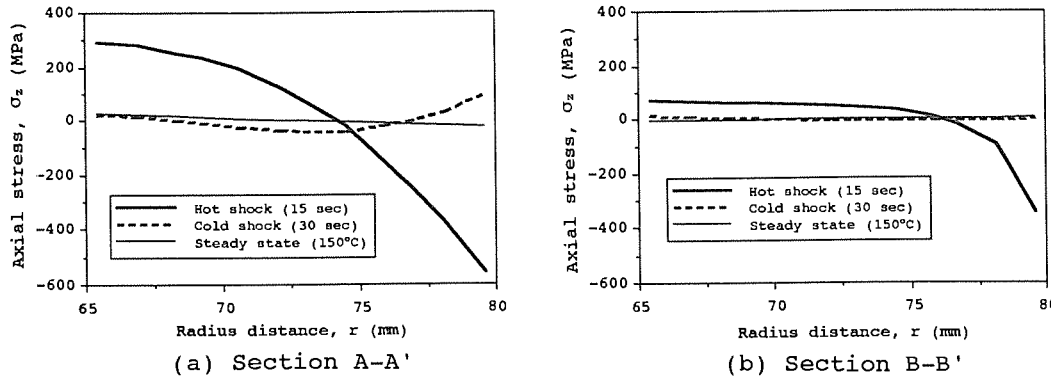

Fig. 5. Stress distribution changes obtained from elastic thermal stress analysis for the hot shock test conditions

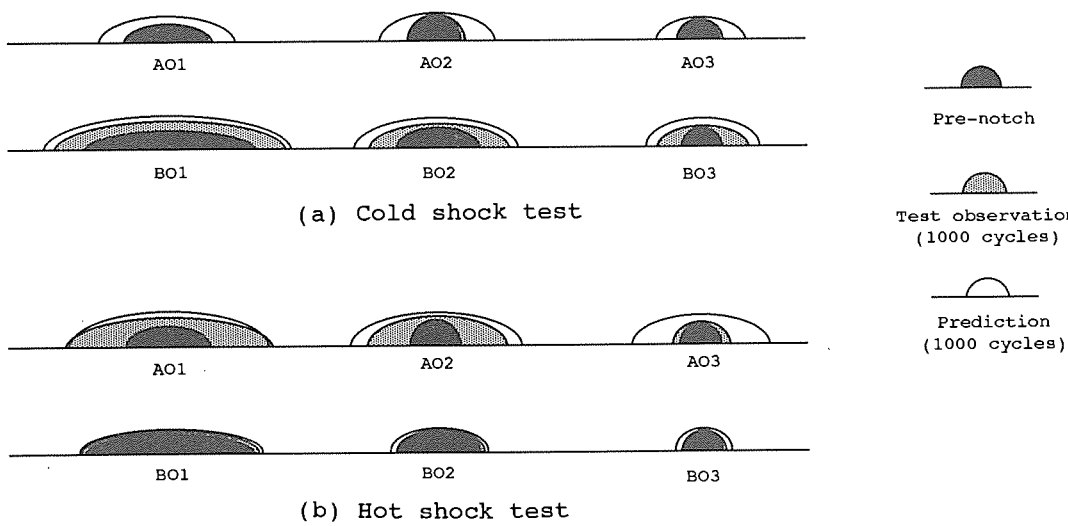

Fig. 6. Comparisons between the predicted crack dimensions and the test observations after 1000 cycles of thermal shock